CIGRE SESSION 48

D1-109

Paris 2020

Partial Discharge Analysis in Gas-Insulated HVDC Systems Using Conventional and Non-Conventional Methods

T. GÖTZ[1*], P. WENGER[2], M. BELTLE[2], K. BACKHAUS[1], S. TENBOHLEN[2], U. RIECHERT[3]

[1]Technische Universität Dresden, Germany
[2]University of Stuttgart, Germany
[3]ABB Power Grids Switzerland Ltd, Switzerland

SUMMARY

Gas-insulated systems (GIS) as a part of high voltage direct current (HVDC) links can reduce the space consumption of the high voltage system considerably. Especially on offshore converter platforms for wind park grid connections and in transition stations between different transmission technologies, the space is limited and GIS can be used beneficially.
To ensure a safe and reliable operation during the whole lifecycle, a reliable partial discharge (PD) diagnosis is necessary. The state of the art measurement techniques for AC transmission systems cannot be directly applied at DC voltage stress due to the missing phase relation. Additionally, the PD behaviour of defects is different at DC voltage and experience in diagnosis is lacking. Therefore, this paper presents the analysis of PD measurements in gas-insulated DC systems using conventional and non-conventional methods.
Well-developed measurement methods according to IEC 60270 and using UHF-sensors are complemented by current measurements and optical investigations of the discharges. The focus is on free moving particles and metallic protrusions, which represent common defects in GIS. All time-resolved PD measurements are compared with respect to their amplitude and impulse intervals. It is shown, that free metallic particles in the GIS move differently at DC voltage compared to the well-known AC motion pattern. Consequentially, the measurement signals vary with the particle position. The utilized methods succeeded in detecting only a fraction of the occurring PD impulses. Recorded impulse amplitudes and time intervals between subsequent impulses can vary significantly between all methods. A substantial contribution is made for better understanding PD in GIS under DC voltage stress, by strategically analysing strength and weaknesses of each detection method.

KEYWORDS
HVDC, GIS, PD measurement, metallic protrusion, free moving particle, UHF, IEC 60270, high speed imaging

*E-Mail: Thomas.Goetz1@tu-dresden.de

1 Introduction

Gas-insulated systems (GIS) benefit from space-saving installations, high reliability and minor dependency from environmental conditions. They are used since the early 1960s for AC transmission [1]. A modern and sustainable energy transmission system requires the usage of high-voltage direct current (HVDC) systems in order to reduce transmission losses across long distances, build interconnectors between independent AC grids and connect offshore windfarms to the existing grid. Nowadays HVDC GIS combine the benefits of HVDC transmission systems and the long operation experiences of AC-GIS, but they are still not prevalent due to the challenges during the development of high-voltage DC equipment [2,3]. GIS can reduce the size of offshore converter stations up to 10 %, are advantageous as transition station between different transmission technologies like overhead-lines (OHL) and cables, cables and GIL or between cables from different manufacturers. Additionally, they are necessary to develop an offshore HVDC grid [4]. In the urban area, their small visible impact and footprint is advantageous compared to air-insulated systems.

Type tests, routine tests and on-site commissioning tests ensure the safe and reliable operation during the entire operation lifetime of all high-voltage equipment including GIS. Partial discharge (PD) measurements are performed in AC-GIS in order to detect critical defects like floating contacts, moving particles, protrusions or voids in the bulk insulation of spacers [5]. PD measurements according to IEC 60270 [6] are performed during all standard tests. Additionally, PD monitoring during service using the ultra-high frequency (UHF) method is state-of-the-art, at least for critical AC infrastructure [5,7].

However, PD measurement and diagnostic under DC voltage stress underlies additional challenges compared to AC voltage. The missing phase relation prohibits standard diagnostic methods like phase resolved PD patterns, which increases the complexity of the PD diagnostic [8]. Pulseless discharges can occur on protrusions in dependence of the gas-pressure and voltage polarity [9], which cannot be detected with conventional partial discharge measurement techniques due to their operating principle. Generally, the discharges at DC voltage stress show a high volatility and can incept and extinct within several minutes or hours [10]. The motion of free moving conductive particles is different compared to AC voltage stress due to the constant electrical field [11].

These challenges are already pointed out in the interim report of CIGRE WG D1.63 [12]. Even though only one defect is assumed in this consideration, since signal separation is not state of the art under DC voltage stress it is hard to detect partial discharges in HVDC-GIS (Table 1). One major problem is the lack of experience.

Table 1 : Relative effectiveness of PD measurement techniques during factory acceptance tests (FAT) and site acceptance test (SAT) concerning defect recognition in HVDC-GIS [12]

Defect	IEC 60270 (FAT)*	UHF (SAT)*
Metallic protrusion	-	-
Moving Particle	-/+	-/+
Floating electrode	-	-
Void	-	-
Particle on insulation	-	-

Index: +|-…effective | less effective …*Assumption due to lack of experience

Therefore, the aim of this paper is to present results of PD analysis in gas-insulated systems under DC voltage stress. Using measurements based on IEC 60270, in the UHF range, optical investigations and PD current measurements the investigations focus on free moving particles and metallic protrusions. Derived from the experimental results, the reliability of currently used PD measurement systems will be assessed for the usage in gas-insulated HVDC systems. Challenges during the measurements will be addressed. Proposals regarding test procedures and test times drawn from this practical experience are elaborated.

2 Experimental and measurement setup

Greinacher circuits supply the test arrangements with high DC voltage. The ripple factor δu is ≤ 3 % according to IEC 60060-1 [13]. The voltage measurement is performed using a calibrated resistive voltage divider. The experiments are carried out in commercially available GIS compartments with an absolute SF_6 gas pressure of p_{abs}=0.5 MPa at 20 °C. The measurements are using an oscilloscope with an analogue bandwidth of at least 3.5 GHz (sampling rate 20 GS/s). The utilized UHF-sensors are similar to the ones presented in [14]. For every investigated PD source, a special electrode arrangement is designed.

2.1 Setup for moving particles

The experimental section consists of commercially available HVDC-GIS components, which form a horizontal, coaxial electrode configuration (Figure 1).

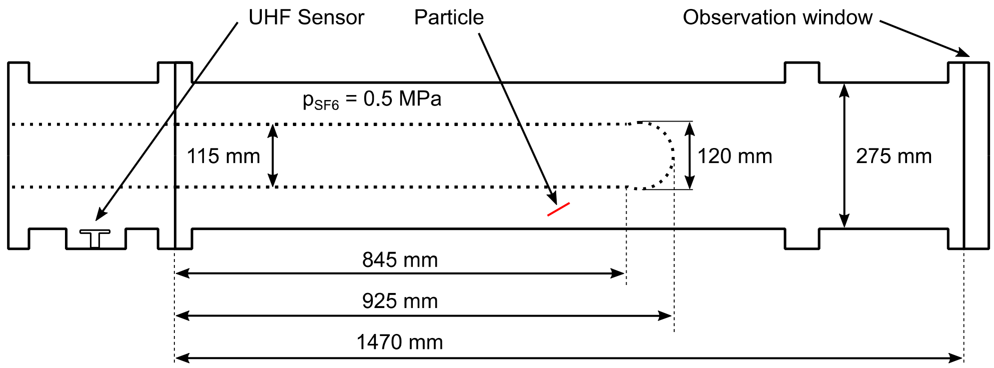

Figure 1: Horizontally aligned coaxial electrode arrangement

Both electrodes, enclosure and inner conductor are made of uncoated aluminium. Particle motion can be tracked with a high–speed camera through an observation window, which is flanged onto the compartment enabling a view axially aligned with the inner conductor. Particle-triggered PD activity is recorded by an UHF measuring system. The UHF-sensor is flanged onto the adjacent GIS compartment, which is separated by a closed support insulator. The sensor output signal is measured with the sampling oscilloscope. However, a protection circuit with a band pass filter characteristic ranging from 100 MHz to 2.2 GHz is applied. In order to achieve time synchronized measurements, the oscilloscope triggers the camera system. Three different particle geometries (Table 2) are investigated in order to correlate particle motion with particle mass and shape.

Table 2: Geometry and material of investigated particles

Geometry	Material	Dimension
Lamella	Aluminum	Length = 2 mm; Width = 1.5 mm; Height = 0.1 mm
Cylinder	Nickel-chromium; Aluminum	Length = 4 mm; Diameter = 0.3 mm
Spiral	Nickel-chromium; Aluminum	Length = 3 mm; Diameter = 0.9 mm

2.2 Setup for metallic protrusions

The weakly-inhomogeneous electrode arrangement of a gas-insulated system is modelled by a sphere-plate electrode arrangement with a gap distance d = 60 mm (Figure 2). At the sphere electrode a high grade steel needle (100Cr6) with a length of l = 5 mm is fixed. The tip radii of the protrusion is about 22 µm. The needle is separated from ground potential using a PTFE-sleeve in order to have the possibility to measure the partial discharge current I_{PD} directly.

The current measurement is performed using a 50 Ω terminating resistor directly at the oscilloscope. In order to have a high signal-to-noise-ration (SNR), the experimental setup is placed in a shielded room.
Measurement circuits according to IEC 60270, using UHF-sensors and using the optical emission of partial discharges are implemented in the experimental setup to compare the sensitivity of the most common measurement techniques with the measured partial discharge current. To perform measurements based on IEC 60270 a coupling capacitor with a capacitance $C_K = 0.5$ nF is attached to the DC voltage supply using an inductor ($L_s = 90$ mH, $R_s = 106$ kΩ). The coupling device (LDIC LDM-5) is in series to the coupling capacitor and directly connected to the amplifier of the PD-measurement system (LDD-5). The integrated amplifier with an upper cut-off frequency of ≥ 30MHz has a gain of 30 dB. The output signal of the amplifier is directly connected to the oscilloscope. In contrast to the instructions in IEC 60270 no additional band-pass filter is used. The noise floor of the calibrated measurement circuit is 0.6 pC.
Below the electrode arrangement the mentioned UHF-sensor is placed. In order to achieve a high SNR a 30 dB amplifier (SwissMains GMS-IV) is placed directly at the output of the UHF-sensor. A surge protector is placed between UHF-sensor and amplifier (SwissMains LPB).
An optical investigation of the partial discharge activity is possible using an observation window, which is flanged onto the compartment enabling a perpendicular view to the protrusion. In front of this observation window a photo-multiplier-tube (PMT, Hamamatsu H11901P-110) is placed. This multiplier-tube is chosen due to its high sensitivity in the UV range. The output signal is directly measured with the oscilloscope.
Due to the limited number of input channels of the oscilloscope either the IEC 60270 signal or the optical signal is measured in addition to the PD current, the UHF signal and the applied DC voltage.

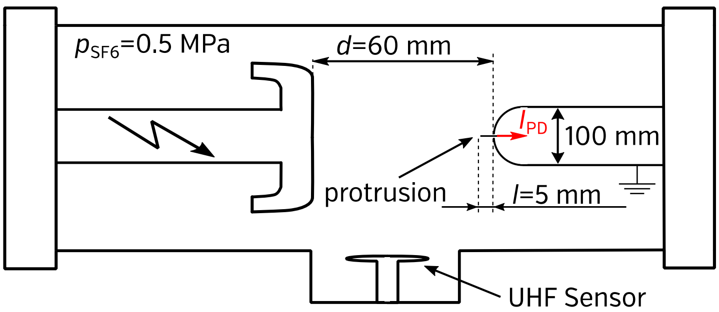

Figure 2: Weakly-inhomogeneous electrode arrangement with fixed needle on ground potential as protrusion

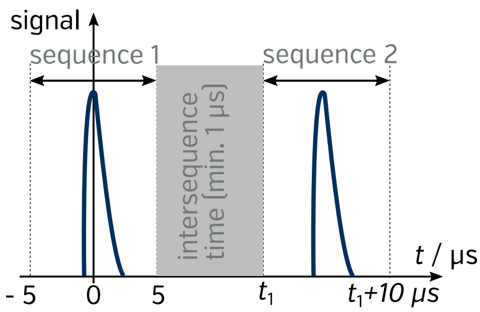

Figure 3: Sequence mode with two sequences

Due to the fact, that the measurement of the partial discharge current requires a high bandwidth of the measurement system [15] and the possibility of rather high time differences between subsequent partial discharge impulses the sequence mode of the oscilloscope is used(Figure 3). One sequence has a duration of 10 µs, the intersequence time depends on the time between subsequent discharges (trigger events) and has a minimum duration of 1 µs.
One sequence includes the simultaneous measurement of all four channels and at least one partial discharge impulse. The presented measurement results are achieved by the evaluation of 2000 sequences.

3 Results

3.1 Moving particle

In AC-GIS free moving particles can be detected using acoustic sensors, which are placed on the enclosure, to detect the mechanical impact of the particles [16]. In combination with conventional measurements and signal processing, their mass and geometry can be estimated [17]. However, under the influence of a high constant electrical field particles tend to perform firefly motion primary at the inner conductor, if energized with negative voltage [18]. This specific defect cannot be detected by acoustic sensors, due to the high damping of acoustic signal along the propagation path through the gas or insulators. However, the UHF measuring technique is suitable to detect most of the variations of motion patterns in combination with a good SNR. Metallic particles in the millimetre range can be detected reliably.

3.1.1 Correlation of particle motion and UHF-PD-signal

The motion of particles can be differentiated into fundamental patterns with respect to the bouncing amplitude and PD signal. Particle geometry, mass and material composition and external parameters, such as gas pressure, applied voltage and polarity and prevailing local charge accumulation influence the particle lift-off and motion. Charge carriers accumulate on the surface of a particle resting on the enclosure. If the resulting force $F_{res} = QE\text{-}mg$ on the particle is positively orientated towards the inner electrode, the particle lifts-off. With applied AC voltage, the particle oscillates with a frequency of 50/60 Hz in vicinity to the enclosure for long periods up to hundreds of milliseconds and rarely crosses the gas gap completely [19]. Particle trajectory of free moving particle are given in Figure 4. The trajectory under AC field condition (blue) is based on results given by Nojima et al. [19]. Particle trajectory under DC field condition (red) is obtained by evaluation of recordings of the high speed camera.

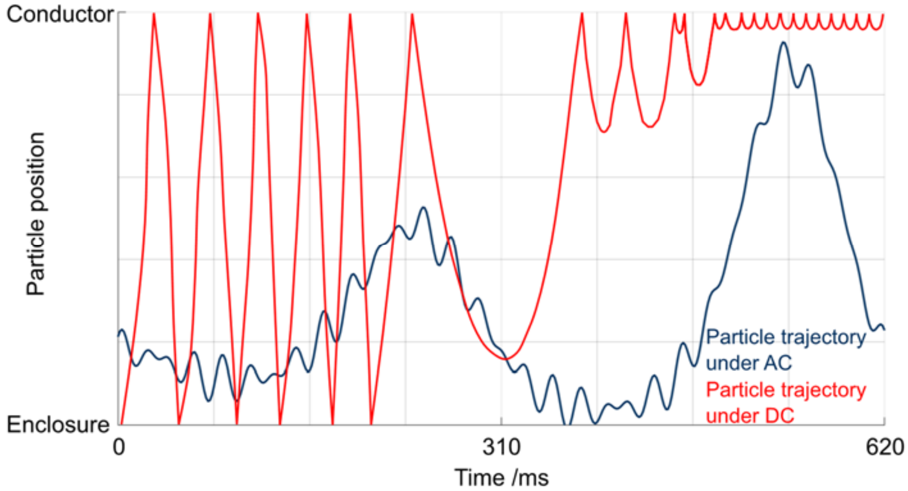

Figure 4: Particle trajectory in the gas gap with respect to the applied voltage waveform

Under DC conditions, particle motion is more diffuse. Immediately after lift-off particles cross the gas gap and strike the inner conductor, if energized with negative DC voltage. Shortly before the contact a PD signal can be detected for the first time. During crossing no PD signal can be detected, neither with conventional, nor with UHF measurement technique. After being repelled from the inner conductor, the recharged particle continues its trajectory back to the enclosure, where it is again recharged and repelled (Figure 5). PD pulse amplitudes, which are recorded while the particle is in close vicinity to the inner conductor exceeds PD amplitudes occurring while the particle is nearby the enclosure up to an order of magnitude. Hence, the location of the particle can be discriminated by the PD signal amplitude.

Bouncing between the electrodes is considered critical to the insulation strength of the gas gap. Particle triggered breakdown of the gas gap has been observed with all particle geometries and materials investigated. In general, small and light particles are less critical, because the distortion of the electric field is lower and the particles convey less hetero-charges to the electrodes. Moreover, space charge regions generated during firefly motion homogenize the local electric field, similar to the corona stabilisation effect at negative protrusions. Large, heavy particles lift off at higher voltages and convey higher amounts of charge to the oppositely charged electrode causing a high field distortion.

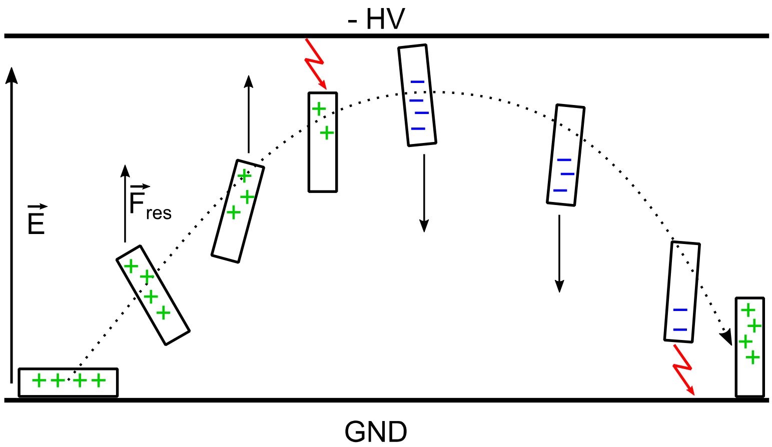

Figure 5: Particle lift-off and oscillation motion under constant electrical field

With increasing electric field strength, the bouncing motion turns into firefly motion. The rapid oscillation at one electrode is accompanied by high PD repetition rates and light emission at the particles' tip. During transition of the different motion patterns, the particle often is observed performing large bouncing at one electrode, within which it almost reaches the opposite electrode, but is accelerated back before contact (Figure 4). Firefly occurs usually at the negative electrode, independent on the polarity of the applied voltage to the inner conductor. However, it is also observed at a positively charged inner conductor in rare occasions [20]. Several distinct modes of firefly are known, which can be discriminated by the maximum clearance between particle and electrode. In general, the smaller the bouncing amplitudes, the more stable the firefly motion. The bouncing amplitude is closely linked to the generation and shape of the space charge region, which is formed by gas ions generated from the discharge activity at the particle. Figure 6 shows the correlation of particle position with respect to the high voltage electrode and the UHF-PD-signal pattern during firefly motion.

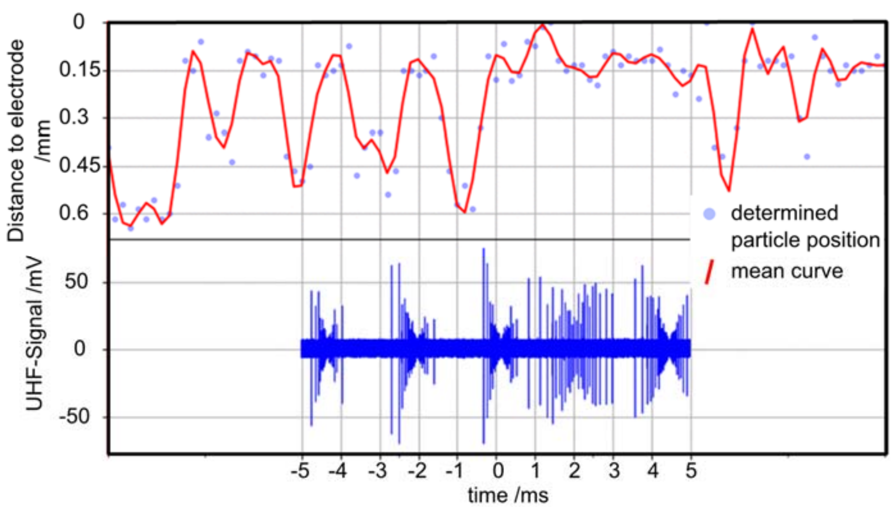

Figure 6: Correlation of particle position with respect to the electrode and UHF-PD-signal during firefly motion of a 4 mm cylindrical particle made of nickel-chromium at E_{mean} = 3.5 kV/mm

In order to derive the particle position from camera frames a MATLAB algorithm is implemented. However, in order to achieve high framerates the high-speed camera image resolution is low (e.g. 320x240 pixel at approx. 15000 fps [21]). Hence, the particle trajectory given in Figure 6 is subject to slight deviations of the actual particle position.
Nevertheless, the evaluation provides evidence that the V-shape pulse sequence occurs, if the particle approaches the inner conductor. The closer the particle gets to the electrode, the smaller the PD pulse amplitude and the higher the PD pulse repetition rate on average. By the time the particle touches the electrode, no further PD pulses are measured. The PD pulses re-occur, as soon as the particle leaves the electrode. If a specific distance from particle to electrode is exceeded no PD pulses arise [11]. Occasionally, particles are observed hovering motionless or with slow locally restricted oscillations in the gas gap. It is assumed, that the permanent exchange of charge carriers between particle and local space charge regions results in a fragile equilibrium of the acting forces on the particles. However, no UHF signals can be detected during this motion pattern.
PD signals of subsequent impulses at small bouncing firefly motion can be as low as 1 µs. Rise times in the range of 1 – 20 ns are observed. Peak-to-Peak pulse amplitudes up to 200 mV are recorded. In the centre of the V-shaped pulse cluster, signal amplitude as low as the noise level are recorded. Moreover, by applying advanced post-processing tools, such as cross-correlation, more PD pulses can be distinguished in the noise, while the particle is about to contact the electrode. Hence, fast sampling and high resolution PD measuring equipment with low SNR is necessary in order to correctly record the PD pulse stream.

3.1.2 Particle deformation during motion

The repetitive mechanical elastic impact at the electrodes and thermal burn-off due to partial discharges at the particles' tip deform the particle and slightly increases the radii of the tip (Figure 7). The mobility of cylindrical-shaped particle changes due to the deformation and the unevenness of the deformation, which can decrease the AC withstand voltage [22]. Moreover, the angel of incidence and hence, the amount of energy which is converted from kinetic energy to rotational energy changes due to the chamfered tip. However, under DC voltage application no significant change of motion pattern of cylindrical -shaped particle is observed. The motion pattern of more complex particle geometries such as spiral and disc-shaped particles are more influenced by the change of dimensions. Spiral-shaped particles are compressed and sometimes break apart, which both alters the motion immediately. Thin rectangular and rectangular-shaped disc particles are transformed to elliptical and circular geometries (Figure 8). Circular discs and spheres don't perform firefly motion, presumably because the lack of a distinct direction of discharge generate low density space charge regions.

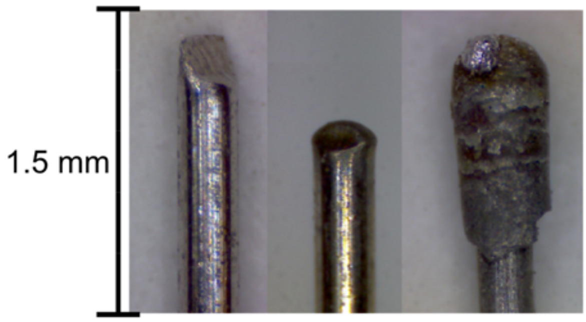

Figure 7: *left:* Tip of cylindrical-shaped particle before motion is initiated, *middle:* particle deformation after firefly and bouncing motion, *right:* particle deformation after particle triggered breakdown

Figure 8: *left:* Disc-shaped particle geometry before motion is initiated, *right:* particle deformation after firefly and bouncing motion

3.1.3 Transition from free moving particle to fixed protrusion

In rare cases, free moving particles weld to the electrode during firefly motion and become a fixed protrusion (Figure 9). The necessary conditions prevailing is not yet fully understood, but the transition from a free moving particle to a fixed protrusion can be observed under AC and DC stress. It is assumed, that the shape of the particles' tip, surface roughness and magnitude of the discharge current are of significance. However, the variation of defect type alters the electric field distribution, formation of space charge regions and discharge development, and thus the PD activity. Hence, the requirement for the PD measurement signal is subject to change, which could cause incorrect reading and misinterpretation.

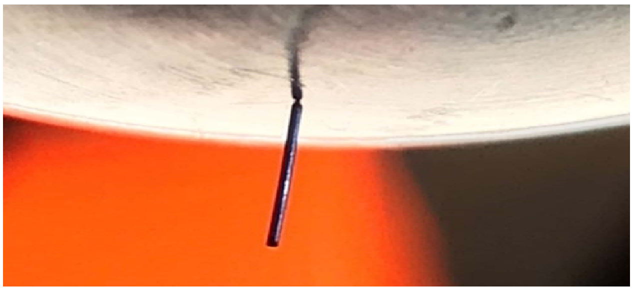

Figure 9: Cylindrical-shaped particle (4 mm) welded on an uncoated high voltage electrode during firefly motion

3.2 Protrusion

A critical length of a protrusion in a coaxial electrode arrangement is in between 1 mm (protrusion at HV electrode) and 6 mm (protrusion at enclosure), depending on the location of the defect [5]. Thus, the protrusion with a length of 5 mm used in this investigation would be critical, independent of its location inside the gas-insulated system. Under AC conditions this type of defect would lead to an apparent charge of a few picocoulomb [5].
To provide an overview about the detectability of a protrusion with different measurement methods the partial discharge current I_{PD} is directly measured at the protrusion (chapter 2.2) and is assumed to show 100 % of the occurring partial discharge impulses. The following three methods will be compared to the current measurement:

- measurement of the apparent charge based on IEC 60270,
- electromagnetic emissions in the UHF range and
- optical emissions.

Due to different measurement ranges selected at the oscilloscope, the minimum detectable impulse current amplitude is $I_{PD\ min\ neg}$ = 20 µA for a negative protrusion and $I_{PD\ min\ pos}$ = -500 µA for a positive protrusion. The measurements are performed at a mean electrical field strength $E_{mean} = U/d$ = 2.2 kV/mm (Table 3). During all presented measurements the voltage is kept constant. The inception voltage U_i is determined with a voltage rising test (dU/dt=0.5 kV/s), the applied voltage at the first measureable current impulse is defined as inception voltage. An analysis of the sensitivity of the measurement systems is presented in chapter 3.2.4.

Table 3: Measurement conditions for positive and negative protrusion

	Inception voltage U_i / kV	Test voltage U / kV	Mean electrical field strength at test voltage E_{mean} / kV/mm	U/U_i
Negative protrusion	44	+ 132	2.2	3
Positive protrusion	77	- 132	2.2	1.7

3.2.1 Ultra-High-Frequency measurements (UHF)

The measurements in the UHF range shall firstly show the main differences between the PD behaviour and the signal amplitude of a free moving metallic particle and a fixed protrusion. One has to keep in mind that the investigations of the free moving particle do not utilize an additional amplifier. The presented UHF signal generated by a protrusion is amplified by 30 dB (factor 1000). The noise level is approximately 10 mV.
The exemplary measurements in Figure 10 show that PD currents of a few milliampere lead to an UHF signal of several ten millivolts. Every measured current impulse leads to an UHF signal. The oscillations after one PD impulse can lead to a non-detectability of impulses with UHF-sensors if the time difference between subsequent PD current impulses is too low.

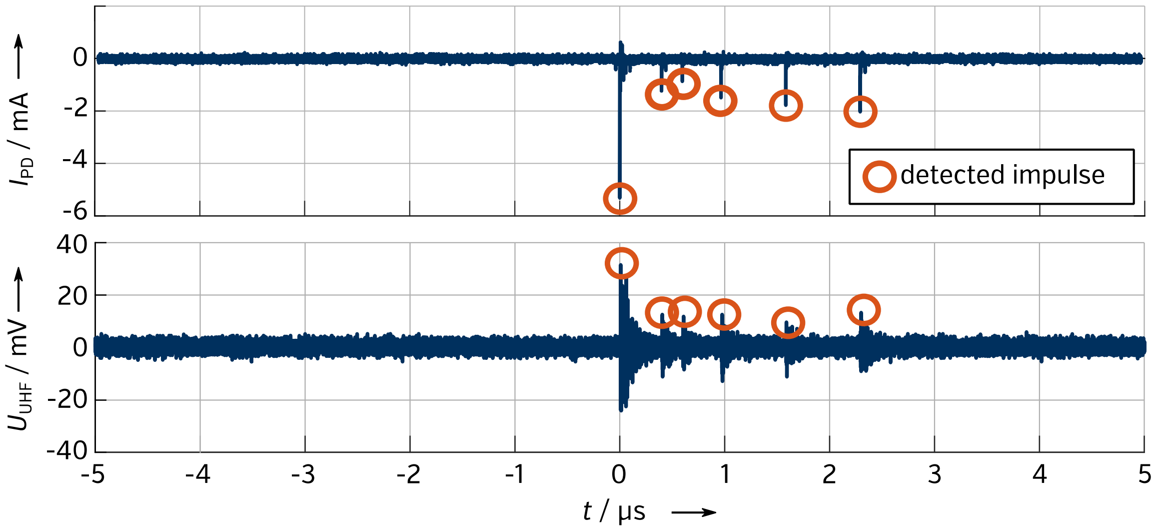

Figure 10: Comparison of PD current measurement at a positive protrusion with PD measurement using UHF range

The evaluation of UHF signals generated by more than 56000 partial discharge current impulses shows that an increasing PD current amplitude leads to an increased UHF signal at a positive protrusion (Figure 11). High partial discharge current impulses can generate low UHF signals and vice-versa. The distribution of the measurement points out, that mainly low signal amplitudes have to be expected. Due to the fact that a high number of impulses is detected close to the noise floor of the UHF measurement system it can be expected, that not every impulse can be detected. Despite the measurements at the negative protrusion are performed at three times the inception voltage, no UHF signal can be measured. This problem can may be avoided if an amplifier with a higher amplification factor would be used.

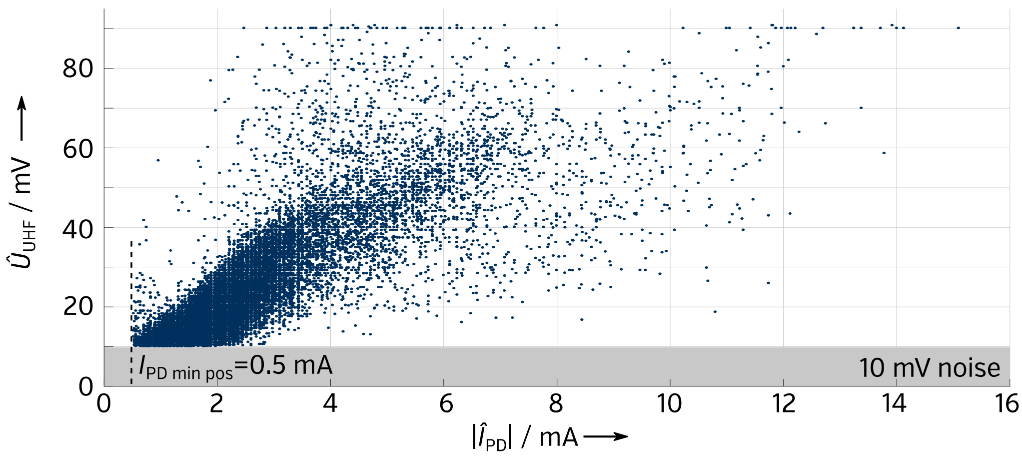

Figure 11: Peak voltage $\hat{U}_{UHF}$ at UHF sensor in dependence of the PD peak current $\hat{I}_{PD}$ at a positive protrusion (maximum measurement voltage $\hat{U}_{UHF,\,max}$ = 90 mV)

3.2.2 Measurement of the apparent charge based on IEC 60270

The identical measured sequence used for the evaluation of the UHF signal is used for the analysis of the measurements based on IEC 60270 [Figure 12]. Longer signal runtimes in the IEC measurements lead to time differences in the occurrence of the signals.
It is obvious that only the impulse with the highest amplitude is detected, with an apparent charge of approximately 1.2 pC. The following five discharges with lower peak current amplitude are lost in the noise.

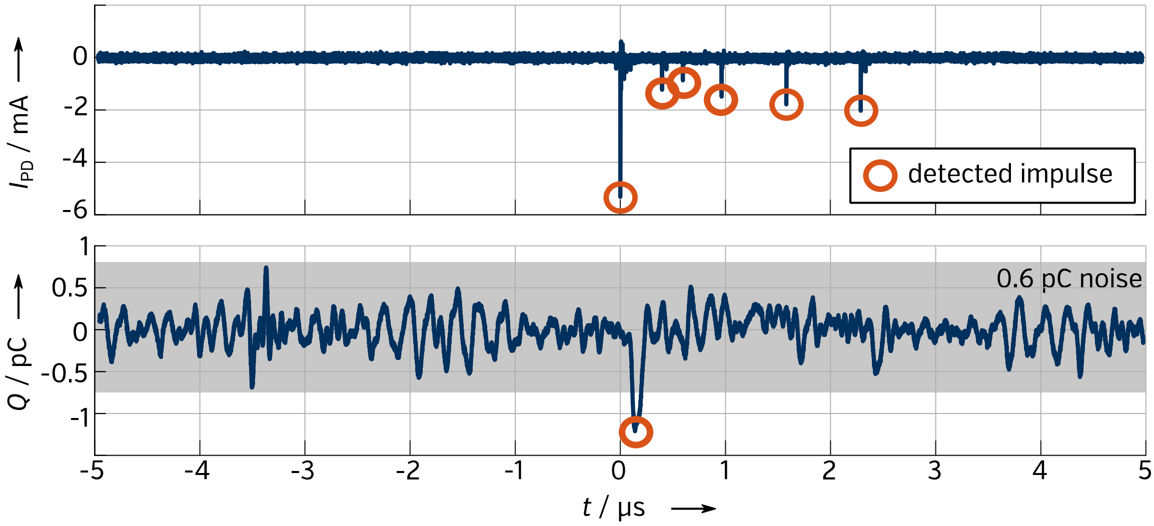

Figure 12: Comparison of PD current measurement with PD measurement based on IEC 60270 at a positive protrusion

Besides the challenge with non-detected, low amplitude impulses it is questionable if commercially available PD-measurement systems would perform a correct counting of the impulses, even if they are outside the noise floor [Figure 13]. If the time difference between two or more subsequent impulses is too low, the output signal of the coupling device does not have a proper time response due to its limited bandwidth [23]. In the presented example three impulses with a high current amplitude would be counted as one single impulse due to their low time difference of approximately 60 ns.

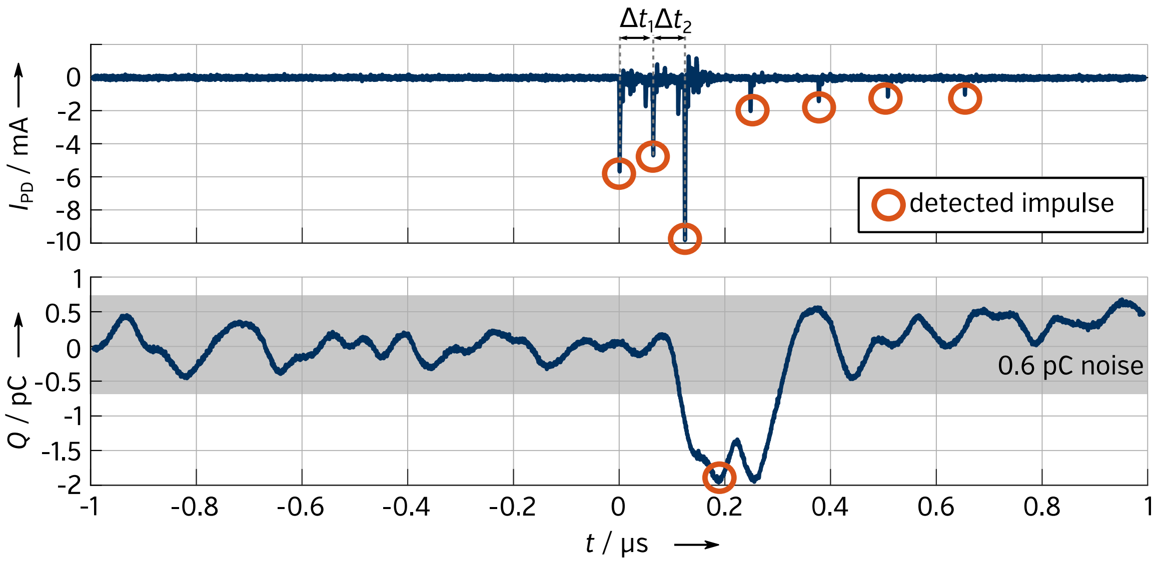

Figure 13: Resolution of subsequent impulses at a positive protrusion with Δt_1 = 64 ns and Δt_2 =60 ns

The measured apparent charge is dependent on the impulse current amplitude (Figure 14). The positive protrusion can generate apparent charges up to 4 pC, but most of the impulses are detected close to the noise floor of 0.6 pC. Hence, it is necessary to have a noise level of less than 1 pC in order to perform a proper detection.
If the polarity of the protrusion is negative, no PD impulse can be detected with measurements based on IEC 60270.
Typical noise levels during SAT tests are 5 pC, and only if a totally encapsulated test circuit is used during FAT a noise level below 1 pC can be achieved [5]. The measurements show, that a positive protrusion cannot be detected reliable, especially during SAT (Figure 14).

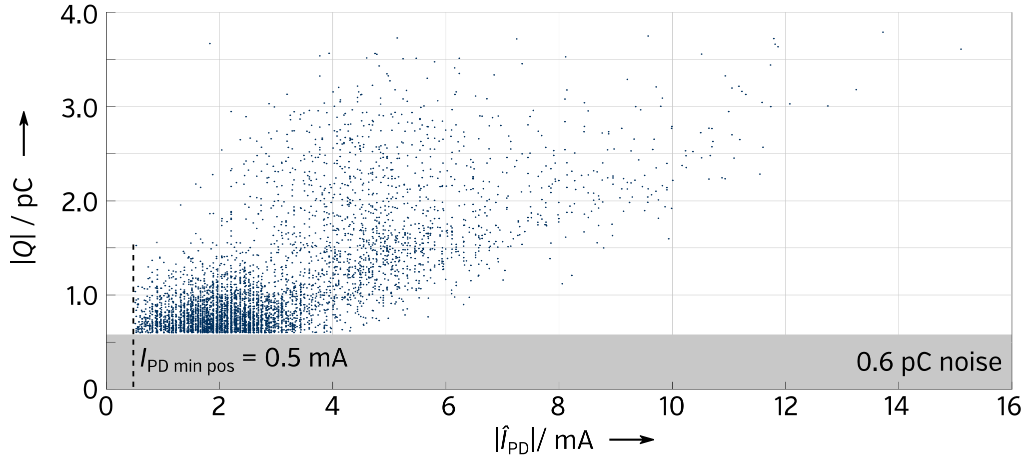

Figure 14: Apparent charge Q in dependence of the PD peak current $\hat{I}_{PD}$ at a positive protrusion

3.2.3 Optical Measurement

As described in chapter 2.2, the optical measurements are performed with a photo multiplier tube (PMT).
The detection of single partial discharge impulses is possible (Figure 15). Nevertheless, if the measured current impulses have similar amplitudes, not every partial discharge event seems to generate an optical emission in the detectable frequency/intensity range.

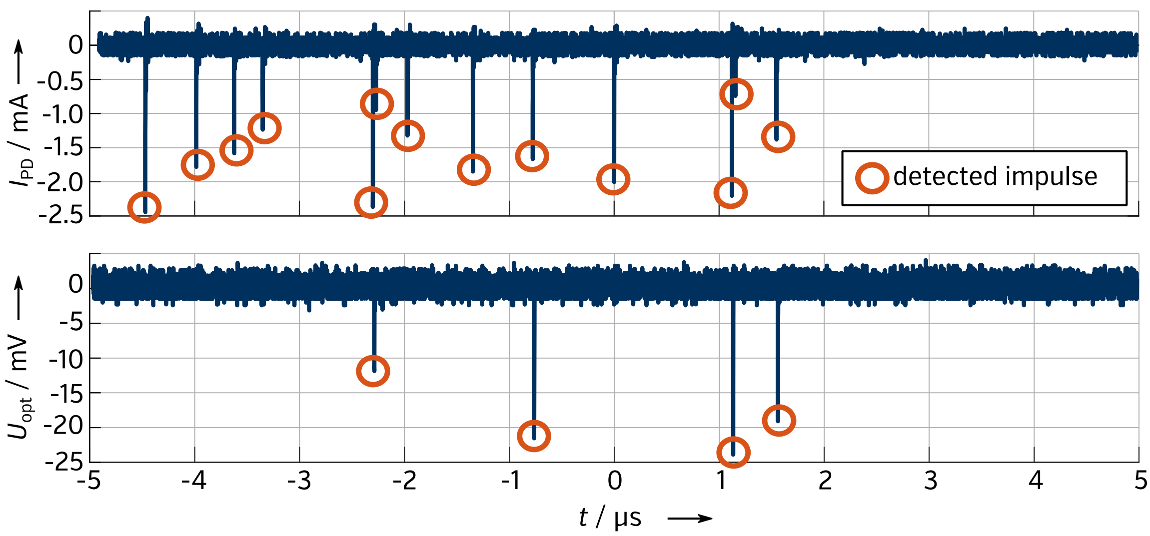

Figure 15: Comparison of PD current measurement with optical detection at a positive protrusion

No apparent correlation can be detected between optical signal strength and partial discharge peak current (Figure 16). Small partial discharge impulses can generate a low optical emission and vice-versa.

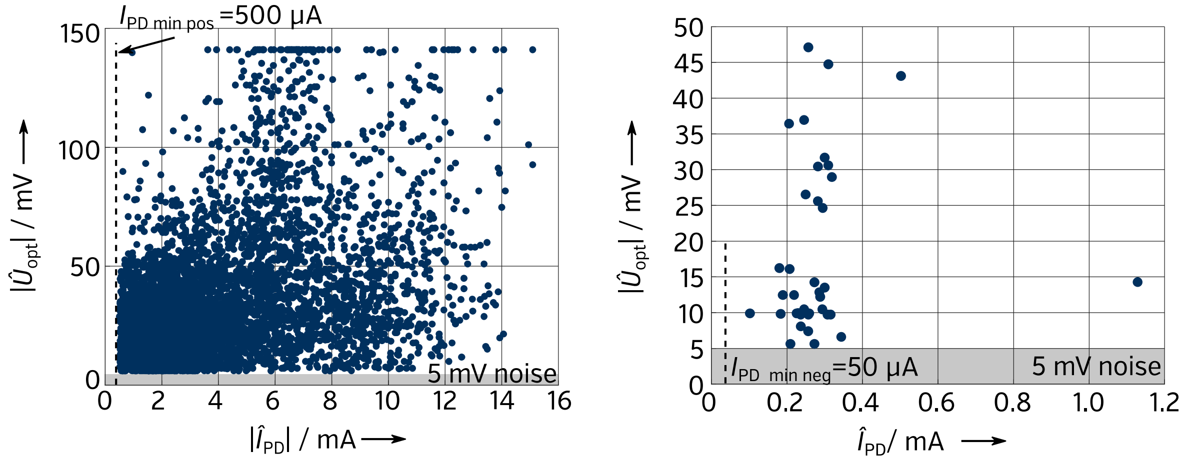

a) Positive protrusion
(measurement range: 0 - 140 mV)

b) Negative protrusion

Figure 16: Peak optical signal $\hat{U}_{opt}$ in dependence of the PD peak current $\hat{I}_{PD}$ at a positive and negative protrusion

In contrast to the measurements using UHF sensors or based on IEC 60270 the optical diagnosis is able to detect a negative protrusion (Figure 16 b)). Once more, it is evident, that the highest peak current is not equivalent with the highest output voltage of the optical measurement system.

3.2.4 Comparison of the results

In order to compare the sensitivity of the used measurement systems the total number of detected impulses is compared. Therefore, all 2000 recorded sequences with a length of respectively 10 µs are evaluated. It is assumed, that the current measurement detects 100 % of the occurring partial discharge impulses and this value is compared with the number of detected impulses by the other measurement techniques (Figure 17).

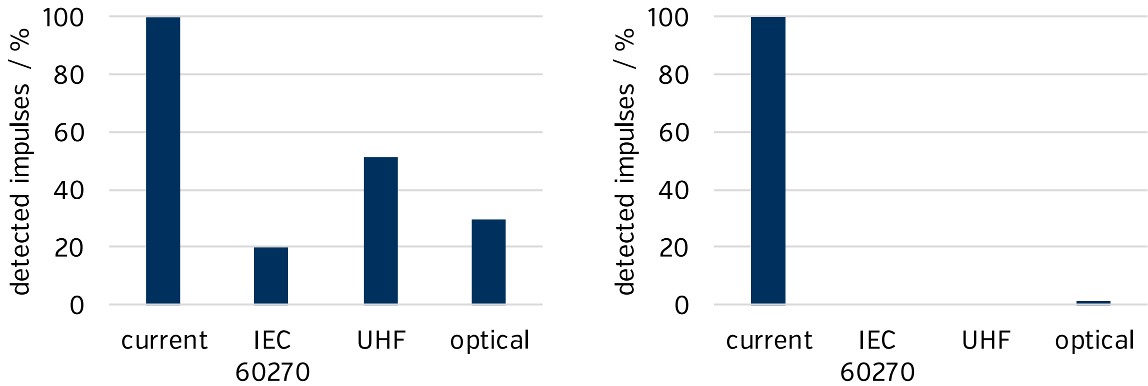

a) Positive protrusion
(out of ≈27000 current impulses)

b) Negative protrusion
(out of ≈3500 current impulses)

Figure 17: Comparison of recognized PD impulses for positive and negative polarity of the protrusion

The positive protrusion can be detected with all measurement techniques. But only 20 – 50 % of the impulses can be detected depending on the measurement method. Consequential, an acceptance criterion using a certain number of pulses with a defined amplitude seems not meaningful under DC voltage stress. Under ideal laboratory conditions, the UHF measurements seems to be the most appropriate detection method. The second most suitable is the optical detection, but it has to be implemented inside a GIS to become relevant for praxis.

As already mentioned in chapter 3.2.1 and 3.2.2 a negative protrusion cannot be detected with the most common measurement techniques, only an optical measurement can detect approximately 1 % of the impulses. This behaviour can clearly be explained if the current amplitudes of a positive and a negative protrusion are compared [Figure 18]. The differences in the peak currents are in the order of one magnitude. Most PD events at a positive protrusion generate peak currents of a few milliampere, whereas a negative protrusion generates peak currents of several hundred microampere. This results in lower signal amplitudes for all measurement systems and therefore in a non-detectability.

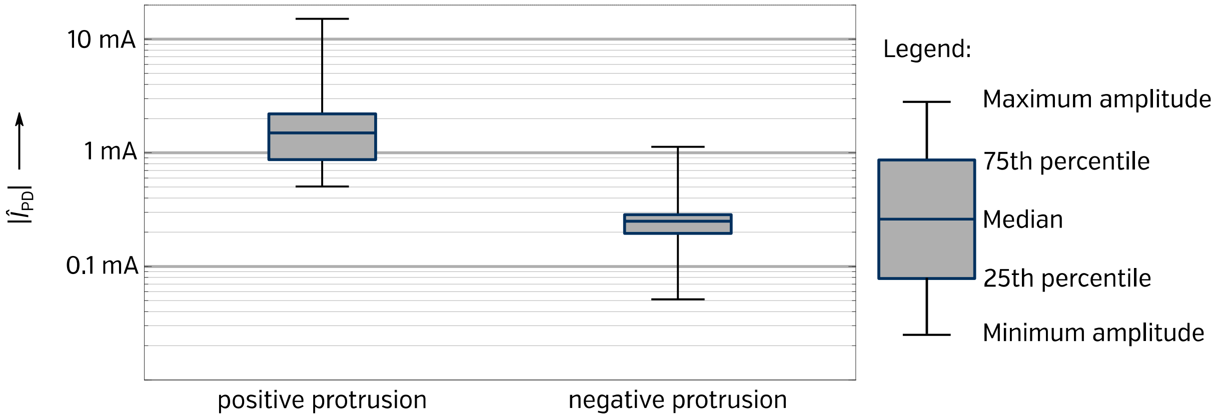

Figure 18: Distribution of the partial discharge peak currents for positive and negative protrusion, derived from 56653 PD impulses at positive protrusion and 6405 PD impulses at negative protrusion

One outstanding factor at a negative protrusion is the permanent direct current flowing with superimposed current impulses [Figure 19]. If this direct current leads to a permanent light emission, it might be useful for PD detection. Therefore the existing optical detection circuit needs to be extended by an amplifier suitable for direct current and high frequency currents if the optical signal would consist out of a constant and a transient component.

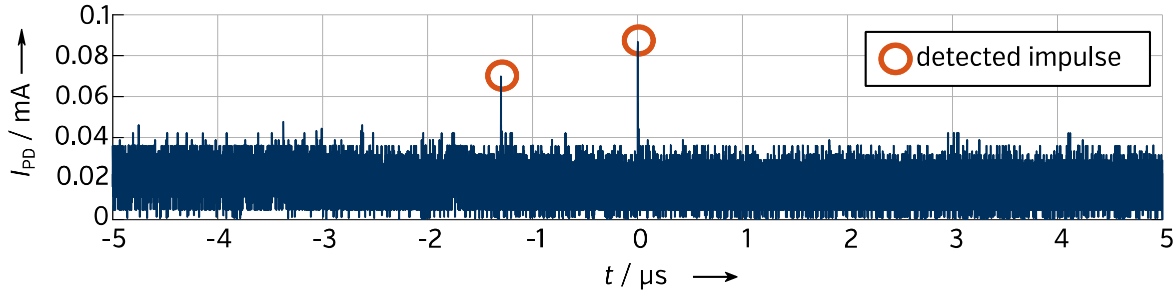

Figure 19: Partial discharge current measurement at a negative protrusion

Comparing the current impulse interval of a negative protrusion [Figure 19] with the distances of a positive protrusion [Figure 15, Figure 17] it can be recognised, that the time difference between subsequent impulses is longer at a negative protrusion. This is also reflected in the number of current impulses detected in the 2000 recorded sequences. At a positive protrusion round about 27000 current impulses are detected, at a negative protrusion only 3500 current impulses are detected within the same number of sequences.

3.3 Comparison of the defects

The signal amplitude of the presented PD sources are given in Figure 20. One has to take into account, that the measured signal amplitude of the positive protrusion is amplified by 30 dB. In order to compare the signal amplitudes of the investigated defects the 30 dB gain used for the UHF-PD-signal of the positive protrusion is deducted. The signal amplitude of a free moving particle is significantly higher than the one of a positive protrusion, and even higher than the one of a negative protrusion, which was not measureable with the experimental setup. Between the two different particle shapes no difference can be seen. Both measurements are carried out under negative polarity, while the particles perform firefly motion at the inner conductor. However, similar results follow from firefly at the enclosure and positive polarity, with similar prevailing electric field strength.

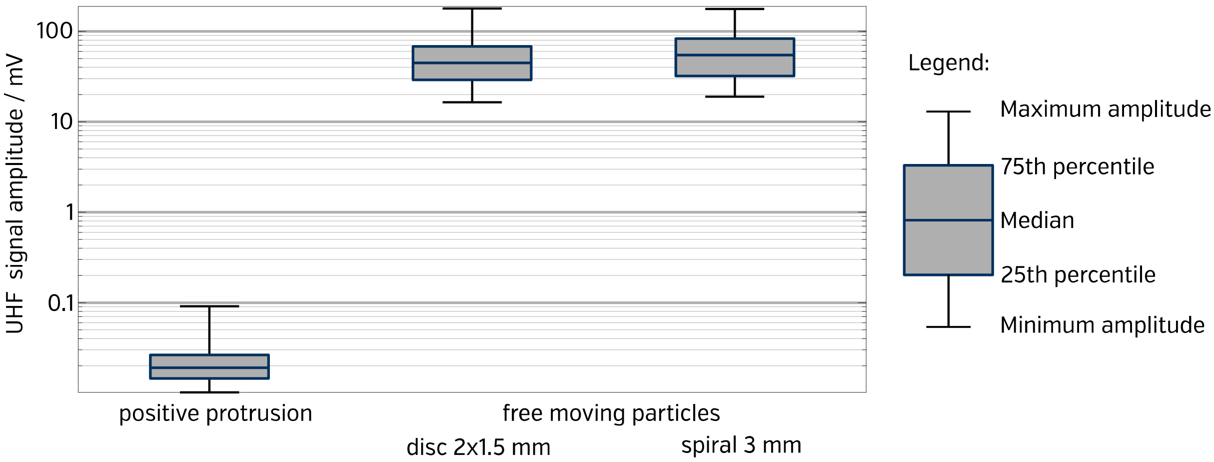

Figure 20: UHF peak signal amplitude of free moving particles and positive protrusion (measurements at the positive protrusion not considering 30 dB gain of the amplifier)

Besides the discussed time domain results, measurements in the frequency domain are equally conceivable (Figure 21). The signal power of a free moving particle is way higher, its frequency range seems broader. This is in agreement with the measurements performed in the time domain and leads to the conclusion that a free moving particles is easier to detect. A more detailed comparison of the measurement results in the frequency domain seems not meaningful, because the transmission paths of the two experimental setups are different and thus can influence the signals [24]. Part of future work will be a more detailed analysis of the signal characteristics of different partial discharge sources in the frequency domain.

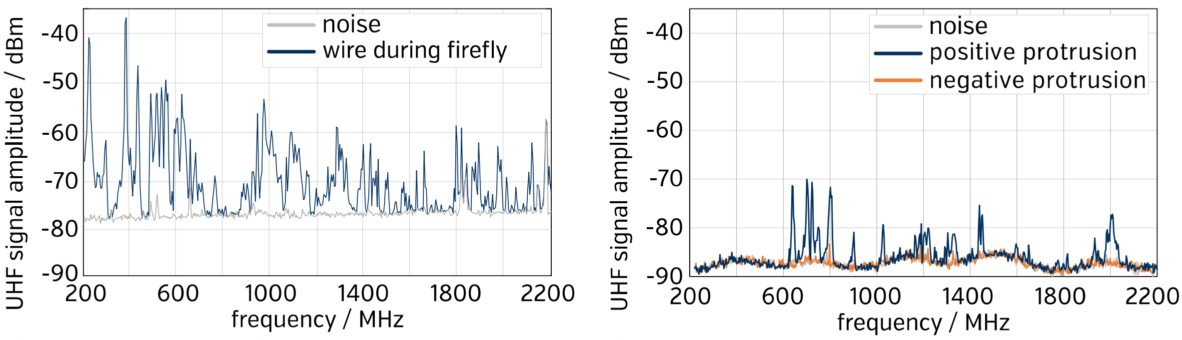

a) Free moving particle (cylindrical-shaped, 4 mm length, E_{mean}=3.0 kV/mm, resolution bandwidth = 2 MHz, sweep time: 100 s, measurement duration: 500 s, max hold)

b) Positive and negative protrusion (E_{mean}=2.2 kV/mm, resolution bandwidth = 10 kHz, sweep time: 99 s, measurement duration: 495 s, max hold)

Figure 21: Frequency spectrum of a free moving particle (measurement w/o amplifier) and a positive and a negative protrusion (measurement with 30 dB amplifier) in comparison to the noise floor

4 Conclusion

The presented results once again underline, that partial discharge measurement under DC voltage stress is a challenge. Due to the constant electrical field, the motion of a free metallic particle is different compared to AC voltage stress. Moreover, applied DC voltage leads to a different PD behaviour at a protrusion. This results in different detection probabilities, depending on the polarity of the applied DC voltage and the location of the protrusion.
Considering the short time difference between subsequent partial discharge current impulses (Figure 13) and the resulting signal output of a measurement system based on IEC 60270 it is obvious, that a counting of partial discharge impulses seems not meaningful. This is contrary to the existing standards for other high voltage devices [25]. The comparison of the sensitivity of the measurement systems show that the detected number of impulses varies with the used PD measurement method. Hence, it may be useful to combine different measurement methods to get a higher sensitivity.
As already mentioned in different standards the measurements have to be performed with both DC polarities. Under negative DC voltage stress the firefly motion of a free metallic particle at the conductor is more stable and therefore easier to detect and interpret. However, a critical protrusion at the conductor can only be detected under positive DC voltage stress, due to the higher signal amplitudes.
The measurements have to be performed using different time parameter settings at the measurement device. The detection of the impulses of a protrusion requires a time resolution of several microseconds in order to get a reliable double pulse resolution. The detection and meaningful interpretation of a moving particle requires measurements in the range of several milliseconds. Considering an additional source of partial discharges in a solid dielectric, the measurement time should exceed the range of minutes.
The large differences in the signal amplitude of the two investigated defects show, that a partial discharge diagnosis under DC voltage stress may use the signal amplitude amongst other values in order to achieve signal separation.
Derived from the measurement results AC voltage should be applied during FAT and SAT in order to benefit from the experience gained within the last decades. Nevertheless, a measurement under DC condition should be performed to detected partial discharges which do not occur under AC voltage stress [9]. If a PD monitoring is planned for future gas-insulated systems under DC voltage stress, the information gained from this investigations lead to the conclusion that it is beneficial to combine different measurement technologies, e.g. optical and UHF, in order to get a higher sensitivity and be able to detect moving particles as well as positive and negative protrusions.

Acknowledgement

This work is partly funded by the *Deutsche Forschungsgemeinschaft* (DFG, German Research Foundation) – project number 379542208 and ABB Power Grids Switzerland Ltd.

5 Bibliography

[1] CIGRE WG D1.28: *Optimized gas-insulated systems by advanced insulation techniques*, TB 571, CIGRE, Paris, 2014.

[2] R. Gremaud et al., “Solid-gas insulation in HVDC gas-insulated system: Measurement, modeling and experimental validation for reliable operation,” in *CIGRE Session Paris 2016*, D1-101.

[3] M. Hirose et al., “Outline of the Kii channel HVDC link,” in *Power Engineering Society Summer Meeting*, Vancouver, 2001.

[4] U. Riechert et al., “PROMOTioN Project: D15.2 Document on test requirements, procedures and methods”, 2018.

[5] CIGRE WG D1.03: *Risk assessment on defects in GIS based on PD diagnostics,* TB 525, CIGRE, Paris, 2013.

[6] IEC 60270:2000: *High-voltage test techniques – Partial discharge measurements*.

[7] CIGRE WG D1.37: *Guide for partial discharge detection using conventional (IEC 60270) and unconventional methods*, TB 662, CIGRE, Paris, 2016.

[8] M. Hering et al., “Detection of particles on the insulator surface in gas insulated DC systems,” in *Highvolt Kolloquium ‘15*, Radebeul, 2015.

[9] T. Götz et al., “Surface discharges on dielectric coated electrodes in gas-insulated systems under DC voltage stress,” in *VDE Fachtagung Hochspannungstechnik,* Berlin, 2018.

[10] M. Hering et al., “Field Transition in Gas-insulated HVDC Systems,” in *IEEE Transactions on Dielectrics and Electrical Insulation*, vol. 24, no. 3, 2017.

[11] P. Wenger et al., “Combined Characterization of Free-Moving Particles in HVDC-GIS Using UHF PD, High-Speed Imaging, and Pulse-Sequence Analysis,” *IEEE Transactions on Power Delivery*, vol. 34, no. 4, 2019.

[12] A. Abbasi et al., “Interim Report of WG D1.63: Progress on Partial discharge detection under DC voltage stress,” in *CIGRE Joint Colloquium SCA2/SCB2/SCD1*, Janpath / New Delhi, 2019.

[13] IEC 60060-1:2010: *High-voltage test techniques – Part 1: General definitions and test requirements*.

[14] A. Tröger et al., “Sensitivity Evaluation of Different Types of PD Sensors for UHF-PD-Measurements,” in *Condition Monitoring and Diagnosis (CMD)*, Tokyo, 2010.

[15] A. J. Reid and M. D. Judd, “Ultra-wide bandwidth measurement of partial discharge current pulses in SF_6,” *Journal of Physics D: Applied Physics,* no. 45, 2012.

[16] S. M. Hoek et al., “New Procedures for Partial Discharge Localization in Gas-Insulated Switchgears in Frequency and Time Domain,” in *XV. International Symposium on High Voltage Engineering*, Ljubljana, 2007.

[17] H. D. Schlemper and K. Feser, “Estimation of Mass and Length of Moving Particles in GIS by Combined Acoustical and Electrical PD Detection” in *IEEE Conference on Electrical Insulation and Dielectric Phenomena*, San Francisco, 1996.

[18] M. C. Cooke et al., “Influence of particles on AC and DC electrical performance of gas insulated systems at extra-high-voltage,” in *IEEE Transaction on Power Apparatus*, vol. 96, no. 3, 1977.

[19] K. Nojima et al., “Forces Affecting Metallic Particle Motion in GIS,” in *International Symposium on Electrical Insulating Materials*, Niigata, 2014.

[20] P. Wenger et al., “UHF-PD Measurement and High-Speed-Imaging of Firefly Motion at the Positive Electrode in HVDC-GIS,” in *IEEE Conference on Electrical Insulation and Dielectric Phenomena*, Washington, 2019.

[21] Datasheet: iX Cameras i-Speed 220/221,” from: https://www.highspeed-xtra.de/images/datenblatt/220-221-Datasheet.pdf, 2020-01-30

[22] L. A. S. Mats and A. E. Vlastós, “Time dependence of AC flashover characteristics for particle-initiated breakdown in GIS,” in *IEEE Transaction on Power Delivery*, vol. 4, no. 1, 1989.

[23] A. Pirker and U. Schichler, “Requirements for PD Detection at DC Voltage to Create the NoDi* Patterns,” in *VDE Fachtagung Hochspannungstechnik,* Berlin, *2018*.

[24] G. Behrmann and J. Smajic, “RF PD signal propagation in GIS: Comparing S-parameter measurements with an RF transmission model for a short section of GIS,” *IEEE Transactions on Dielectrics and Electrical Insulation*, vol. 23, no. 3, 2016.

[25] IEC 62199:2004: *Bushings for D.C. application*.